Journal of Lasers in Medical Sciences

J Lasers Med Sci 2026;17:e8

Original Article

http://journals.sbmu.ac.ir/jlms

doi:10.34172/jlms.2026.08

Synergistic Photodynamic Antimicrobial Therapy Using 405 nm Laser Diode and Moringa Oleifera-Derived Silver Nanoparticles against Pathogenic Bacteria

Suryani Dyah Astuti[1*], Agustina Dwi Cahyani[1], Endarko[2], Sri Dewi Astuty[3], Ahmad Khalil Yaqubi[4], Muhammad Nurdin[5], Dezy Zahrotul Istiqomah Nurdin[6], Ardiansyah Syahrom[7]

[1]Department of Physics, Faculty of Science and Technology, Universitas Airlangga, Surabaya/60115, Indonesia
[2]Department of Physics, Institut Teknologi Sepuluh Nopember, Kampus ITS, Sukolilo Surabaya 60111, Surabaya, East Java, Indonesia
[3]Department of Physics, Faculty of Mathematics and Natural Sciences, Hasanuddin University, Makassar, Indonesia, 90245
[4]Center for Biomedical Research, National Research and Innovation Agency (BRIN), Cibinong, 16912, Indonesia
[5]Department of Chemistry, Faculty of Mathematics and Natural Sciences, Universitas Halu Oleo, Kendari, 93232, Indonesia
[6]Department of Radiology Imaging Technology, Faculty of Health and Education, Muhammadiyah Karanganyar University, Karanganyar, 57761, Indonesia
[7]Department of Applied Mechanics and Design, Faculty of Mechanical Engineering, Universiti Teknologi Malaysia, Johor Bahru/81310, Malaysia

***Correspondence to**
Suryani Dyah Astuti,
Email: suryanidyah@fst.unair.ac.id

Received: September 1, 2025
Accepted: November 19, 2025
ePublished: May 2, 2026

Abstract

Introduction: This study examines the antibacterial capabilities of Moringa oleifera green-synthesized silver nanoparticles (AgNPs-MO), in combination with UV light and a blue laser set at 405 nm, against *Staphylococcus aureus* and *Escherichia coli*. Higher concentrations of AgNPs-MO enhanced the antimicrobial activity when exposed to both light treatments. The findings suggest that Moringa oleifera-derived photosensitizers improve the efficacy of photodynamic antimicrobial therapy, offering an eco-friendly approach for enhanced infection control.

Methods: The experimental design comprised four groups: three bacterial groups (A1/A2 and A3/A4) exposed to laser irradiation at varying concentrations and durations of silver nanoparticles, and a control group (T0) that was not exposed to laser irradiation. A photosensitizer produced from Moringa oleifera was also administered to bacteria in groups A2 and A4, and different laser exposure durations were then applied. After incubation, bacterial colonies were measured with a Quebec colony counter.

Results: Statistical analysis using a two-way ANOVA factorial test and post-hoc Tukey test revealed significant reductions in bacterial viability. *E. coli* exhibited viability reductions of 70.90%, 76.44%, and 79.87% with mmol L-1, mmol L-1.5, and mmol L-2 AgNPs-MO after 180 seconds of laser exposure, respectively. Similarly, *S. aureus* showed viability reductions of 97.48%, 95.94%, and 94.72% under the same conditions.

Conclusion: At an energy density of 3.44 J/cm^2, our approach demonstrated notable efficacy, achieving a 79.87%±1.92% inactivation of *E. coli* and a 97.48%±0.78% inactivation of *S. aureus*. This study suggests promising applications for the combined use of a blue laser, UV radiation, silver nanoparticles, and Moringa oleifera extract in combating infectious bacteria.

Keywords: Photoinactivation, Photosensitiser, Blue laser, *Escherichia coli*, *S. aureus*

Introduction

Antibiotic-resistant bacterial infections are a growing public health concern, particularly in Indonesia, where *Staphylococcus aureus* (*S. aureus*) and *Escherichia coli* (*E. coli*) contribute significantly to morbidity and mortality.[1] For example, the mortality rate from diarrhea reached 3.04% in 2016.[2,3] While new antibiotics continue to be developed, their production is expensive and often environmentally harmful, motivating the search for cost-effective, eco-friendly alternatives.[4]

Nanotechnology offers a promising approach, allowing the manipulation of materials at the nanoscale (1–100 nm) to inhibit or kill bacteria without harming healthy tissues.[5,6] Silver nanoparticles (AgNPs) are especially attractive due to their unique physicochemical properties, high surface area, and ability to bind biomolecules.[7] Other noble metal nanoparticles, such as gold (AuNPs), palladium (PdNPs), and platinum (PtNPs), also exhibit antimicrobial properties, but AgNPs are widely used because of their effectiveness and biocompatibility.[8,9]

Please cite this article as follows: Astuti SD, Cahyani AD, Endarko, Astuty SD, Yaqubi AK, Nurdin M, et al. Synergistic photodynamic antimicrobial therapy using 405 nm laser diode and Moringa oleifera-derived silver nanoparticles against pathogenic bacteria. J Lasers Med Sci 2026;17:e8. doi:10.34172/jlms.2026.08

Nanoparticles can be synthesized via top-down methods, such as milling and laser ablation, or bottom-up approaches, including chemical reduction, sol-gel processes, and green synthesis.[10,11] Green synthesis using plant extracts is particularly advantageous, offering an environmentally friendly, cost-effective method where plant phytochemicals serve as reducing and stabilizing agents.[12] AgNPs produced this way often show enhanced antibacterial activity due to bioactive compounds such as flavonoids, terpenoids, and tannins.[13,14,15]

Moringa oleifera leaf extract has been demonstrated as an effective reducing agent for AgNP synthesis.[16] Its phytochemicals not only stabilize nanoparticles but also contribute antibacterial, anticancer, and hypotensive properties.[17, 18] The antibacterial activity of AgNPs depends on multiple factors, including particle size, shape, concentration, bacterial species, and interaction duration.[19–20] Silver nitrate ($AgNO_3$), commonly used as a precursor, also influences nanoparticle size and efficacy.[21]

Photodynamic Inactivation (PDI) combines a light source with a photosensitizer to produce reactive oxygen species (ROS), which damage bacterial cells without harming healthy tissues.[22–23] Blue light (400–500 nm), particularly at 405–450 nm, is effective for activating photosensitizers like AgNPs, enhancing their antibacterial activity.[24] Previous studies have demonstrated that AgNPs activated by a 450 nm diode laser can significantly reduce microbial survival, suggesting potential effectiveness against *S. aureus* and *E. coli.*[25]

The aim of this study is to investigate the antibacterial properties of green-synthesized AgNPs from Moringa oleifera leaves when activated by blue laser irradiation. The study evaluates the synergistic effects of AgNPs and blue light for photodynamic antibacterial therapy, with a focus on their efficacy against *S. aureus* and *E. coli*.

Materials and Methods

Preparation and Synthesis of Moringa Oleifera Silver Nanoparticles

The study explored the use of Moringa leaves as natural materials to produce silver nanoparticles (AgNPs-MO). The process involved drying and crushing the leaves dissolved in ethanol and water, heating the solution, centrifuging, and adding more ethanol-water solvent. The leaves were well-washed, arranged in a single layer, rotated, and ground into a fine powder. An environmentally friendly synthesis method was used, with Moringa leaf extract as the reducing and stabilizing agent. The effects of three different amounts of silver nanoparticles on the synthesis process and nanoparticle characteristics were evaluated. The phytochemicals in the extract reduced silver ions to nanoparticles and prevented aggregation, ensuring stable production. The study also treated bacteria with laser irradiation with AgNPs-MO photosensitizer, ensuring proper comparison. Experimental controls were incorporated to ensure proper comparison.

Characterization of AgNPs-MO

Several characterization techniques were employed to confirm the formation and properties of the synthesized nanoparticles. UV–Vis spectrophotometry was used to identify the surface plasmon resonance (SPR) peak, confirming AgNP formation. Particle Size Analyzer (PSA) determined particle size distribution, revealing average diameters of 7.26 nm, 54.01 nm, and 100.74 nm at different concentrations. The study also treated bacteria with laser irradiation using AgNPs-MO as the photosensitizer, ensuring proper comparison. Experimental controls were incorporated to ensure reliable results.

Study Design

To evaluate the effects of several parameters (such as laser irradiation, UV radiation, silver nanoparticle concentration, and photosensitizer treatment) on bacterial photoinactivation, the present researchers used a factorial experimental design with numerous treatment groups. Each treatment group measured the bacterial colony under certain settings, including laser exposure and nanoparticle concentration.

S. aureus and *E. coli* vitality were observed under various treatment circumstances, including changes in the concentration of AgNPs-MO and the length of laser irradiation. The study used statistical analysis to ascertain statistically significant variations among the treatment groups.

Culture of Bacteria

Tryptone Soy Broth (TSB) was used to cultivate the microorganisms *E. coli* and *S. aureus.* The colonies were then cultured for 24 hours at 37°C until they achieved a McFarland standard of 1.0. [20]

Laser Source

Using an OMMOL L-6810B-220V power meter, the blue laser employed in the investigation had a wavelength of 405 nm, a spot beam area of 0.13 cm2, and a power output of 2.49 mW. The laser irradiation for 90, 120, 150, and 180 seconds was applied. Using UV-Vis spectrophotometry with a Jasco CT-10 monochromator, we measured the absorption spectra of the generated silver nanoparticles in order to confirm their characteristic absorption peaks. Using Dynamic Light Scattering (DLS), particle size analysis revealed that AgNPs had diameters of 7.26 nm, 54.01 nm, and 100.74 nm at different concentrations.[25]

$$\text{Energy Density (J.cm}^{-2}\text{)} = \text{Intensity (W.cm}^{-2}\text{)} \times \text{Irradiation Time (s)}$$

Anti-bacterial Activity Test

The disc diffusion method was modified to include UV

irradiation and nanoparticle application to study the antibacterial activity of a material. A 50 µL bacterial culture was distributed on Tryptic Soy Agar, and a paper disc was subjected to UV irradiation to enhance the antibacterial action of 10 µL of Moringa leaf extract with nanoparticles. The disc was then incubated for a day under controlled conditions. The efficacy of AgNPs-MO in combination with a 450 nm laser and UV light was evaluated by examining inhibitory zones surrounding the disc. This improved approach allows for a comprehensive assessment of their combined potential as antimicrobial agents.

Reactive Oxygen Species (ROS) Formation and Quantification

To evaluate the underlying mechanism of antibacterial photodynamic therapy (aPDT), the generation of reactive oxygen species (ROS) during laser irradiation was measured. ROS production was assessed using 2′,7′-dichlorofluorescein diacetate (DCFH-DA) as a fluorescent probe. Briefly, AgNPs-MO suspensions were incubated with DCFH-DA and then exposed to 405 nm blue laser light for 90, 120, 150, and 180 seconds.

After irradiation, fluorescence of oxidized DCF was quantified using a microplate reader (Ex/Em = 485/530 nm). The results were compared between the treated and control groups (no laser and no nanoparticles). An increase in fluorescence intensity indicated higher ROS formation. This quantification confirmed that blue laser-activated AgNPs-MO produced substantial ROS, which play a central role in bacterial membrane damage and inactivation during aPDT.

PDI Treatment

Four groups were created from the samples: the control group (T0), *E. coli* samples (A1 and A2), and *S. aureus* samples (A3 and A4). Bacteria in groups A2 and A4 were treated with AgNPs-MO and exposed to blue laser radiation for 90, 120, 150, and 180 seconds. After treatment, the samples were cultured for a day at 37°C and cultivated on Tryptic Soy Agar (TSA). The number of bacterial colonies was determined using the Quebec colony counter. Group labels were defined to match observation tables and graphs, ensuring consistent incorporation of the research design with observations.

Statistical Analysis

The study utilized IBM SPSS's two-way ANOVA factorial test to analyze the effects of bacterial strain and radiation treatment on bacterial inactivation. It identified the main effects of each element and their interactions across bacterial strains. Tukey's post hoc test was used to examine differences between treatment groups, with statistical significance set at $P < 0.05$. The findings will help determine the most effective radiation therapy for photoinactivating *S. aureus* and *E. coli* microorganisms.

Results

Clinical Assessment

Figure 1a shows the findings of the characterization of the AgNPs-MO absorption spectrum. The UV-Vis absorption spectra were measured in the wavelength range of 325 nm to 525 nm. Notably, Moringa leaf extract exhibits an absorption spectrum spanning approximately 200 nm to 691 nm, which aligns with the use of a blue laser in this study.

Determining the particle size distribution is the goal of the particle size analyser. Infrared scattering is used in PSA's Dynamic Light Scattering (DLS) technique. Spectroscopy photon correlation is another name for DLS. The diameter of the circle of particles that diffuse at the same speed at the time of measurement is used by DLS to determine particle size. The AgNPs-MO mmol L^{-1}, $L^{-1.5}$, and L^{-2} particle size values on day 1 at D90 are 7.26 nm, 100.74 nm, and 54.01 nm, respectively, based on the PSA test. According to this finding, because of their size range

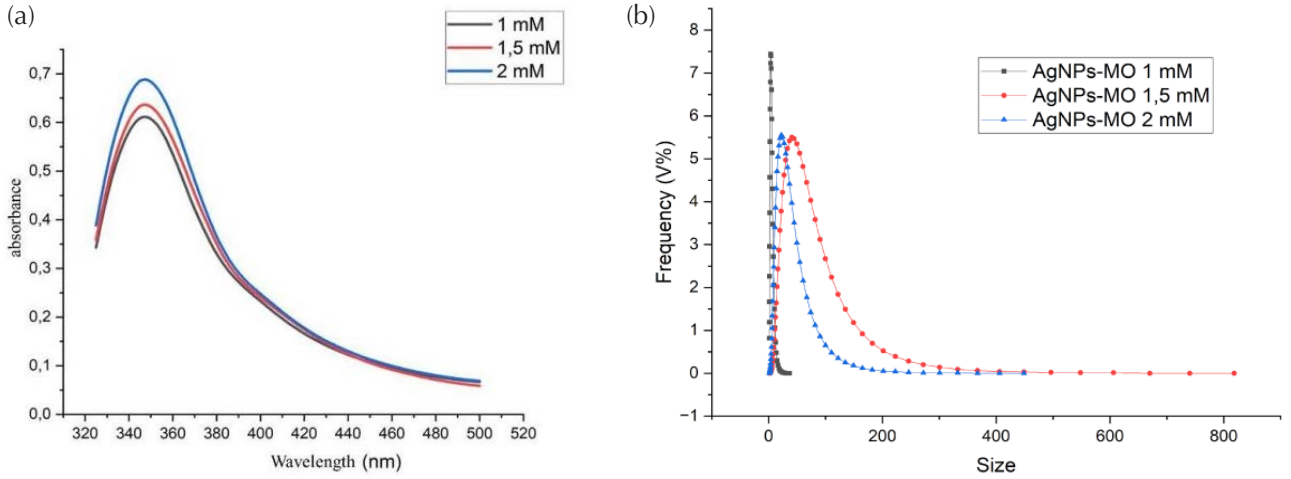

Figure 1. (a) UV-Vis absorbance spectrum of AgNPs-MO at concentrations of mmol L^{-1}, mmol $L^{-1.5}$, and mmol L^{-2}. (b) PSA AgNPs-MO test result at mmol L^{-1}, mmol $L^{-1.5}$, and mmol L^{-2} concentrations

of 1-100 nm, AgNPs-MO mmol L^{-1}, mmol $L^{-1.5}$, and mmol L^{-2} are categorized as nanoparticles. The PSA test results for silver nanoparticles made using AgNPs-MO at three different concentrations are shown in Figure 1b: (a) mmol L^{-1}, (b) mmol $L^{-1.5}$, and (c) mmol L^{-2}.

In this case, silver nanoparticles act as a photosensitizing agent for bacterial inactivation via photodynamic inactivation. The main characteristics of AgNPs-MO as a photosensitizer are the absorption spectrum and particle size, measured by UV-visible spectroscopy and a particle size analyzer. The AgNP absorption spectrum is used to select the wavelength of the laser light source so that appropriate laser energy absorption occurs. Meanwhile, measuring the particle size of AgNP-MO helps determine the surface area available for laser energy absorption, which influences its effectiveness as a photosensitizer in microbial inactivation. Figure 1b shows the PSA AgNPs-MO test result at mmol L^{-1}, mmol $L^{-1.5}$, and mmol L^{-2} concentrations.

The study explored the effectiveness of UV radiation in bacterial inactivation. Researchers used a 30-minute UV radiation exposure with an intensity of 5 mW/cm², focusing on samples exposed to 254 nm for 15 minutes before laser and AgNP-MO treatments. The antibacterial test determined the diameter of inhibition zones against *S. aureus* and *E. coli* using the disc diffusion method. AgNPs-MO produced distinct inhibition zones against *E. coli* at concentrations of mmol L^{-1}, mmol $L^{-1.5}$, and mmol L^{-2}, and showed similar inhibitory effects against *S. aureus*. Higher dosages of AgNPs-MO may cause nanoparticles to aggregate, decreasing their effective surface area and bioavailability, which might explain the reduction in the inhibitory zone for *E. coli*. Figures S1 shows the Antibacterial test results of AgNPs-MO using the disc diffusion method against *E. coli* and Figure S2 shows the antimicrobial test result against *S. aureus*.

There are noticeable variations in the antibacterial activity of AgNPs-MO between *S. aureus* and *E. coli*, with the former showing greater inhibition zones and the latter having smaller inhibition zones. AgNPs-MO considerably suppresses *S. aureus* more than *E. coli*. According to Table S1, the inhibitory zone for *S. aureus* grows when AgNPs-MO concentrations rise, but it falls for *E. coli*, indicating that *E. coli* is less impacted. Table S2 shows particle size of AgNPs-MO at different concentrations.

Adding AgNPs-MO to the two bacterial samples demonstrated the antibacterial properties of the synthesis (Figure S3). The bacterial growth results were calculated by counting the number of bacterial colonies that formed in each well or cup containing AgNPs-MO. The thicker peptidoglycan layer in *S. aureus's* cell wall, which facilitates more efficient interaction with AgNPs-MO and increases antibacterial activity, is what caused the increased inhibition of the germs at higher doses.[6]

The study involved two treatment groups of *E. coli*: one exposed to laser irradiation alone and the other exposed to laser irradiation in combination with 50% AgNPs-MO at each concentration. The observational data were analyzed using IBM SPSS's two-way ANOVA factorial test to ensure they met standards for interval-scale measurements, homogeneity of variances, and normal distribution. The study found that laser treatment with mmol L^{-2} AgNPs-MO for 180 seconds resulted in the highest percentage of E. coli bacterial deaths at 79.86%. The therapy produced distinct energy density for each treatment, and the number of bacterial colonies decreased compared to the control group. The *E. coli* bacterial death percentage varied with the concentration of *S. aureus* bacteria, with the highest percentages at 90, 120, 150, and 180-second intervals. The study suggests that laser treatment with mmol L^{-2} AgNPs-MO can potentially improve bacterial outcomes. The findings showed that these time intervals had considerably different outcomes. The treatment results of the three groups are shown in Figure 2A, which also shows the correlation between bacterial survivability concerning the colony count and the length of the radiation. Figure 2B compares the proportion of bacterial mortality in each of the three treatment groups. Table 1 presents the findings derived from the statistical test results.

Figure 2 shows the decreased viability of *E. coli* treated with AgNPs-MO at different concentrations: (a) mmol L^{-1}, (b) mmol $L^{-1.5}$, and (c) mmol L^{-2}. The figure illustrates the gradual reduction in bacterial viability as the concentration of AgNPs-MO increases. This figure demonstrates the effectiveness of AgNPs-MO in reducing bacterial viability, with higher concentrations showing more significant reductions in bacterial counts.

Table 1 presents the mean bacterial death (%) of *E. coli* under varying concentrations of AgNPs-MO (mmol L^{-1}, mmol $L^{-1.5}$, and mmol L^{-2}), different laser exposure times (90, 120, 150, and 180 s), and their interactions. Each treatment group consisted of N replicates. The highest bacterial death (79.87%) was observed with 180-second laser exposure combined with mmol L^{-2} AgNPs-MO. Results show that both higher concentrations of AgNPs-MO and longer laser exposure times significantly increased bacterial inactivation ($P < 0.05$).

Figure 3 was prepared by treating *S. aureus* bacteria with three concentrations of AgNPs-MO (mmol L^{-1}, mmol $L^{-1.5}$, and mmol L^{-2}) and exposing them to blue laser irradiation for four time intervals (90, 120, 150, and 180 seconds). The study found that laser treatment with mmol L-1 AgNPs-MO for 180 seconds resulted in the highest percentage of *S. aureus* bacterial mortality (97.48%). The energy densities were adjusted for each treatment, and compared to the control group, there were fewer bacterial colonies. AgNPs-MO was added to each change in *S. aureus* bacteria concentration throughout the manufacturing process, resulting in bacterial death percentages of 94.24%, 94.89%, 96.10%, and 97.48%,

Table 1. Results of statistical analysis on *E. coli* bacteria

Treatment	Group	N	Bacterial Death (%)		Conclusion
			Mean	SD	
Concentration AgNPs-MO (mmol L^{-1})	1 (1)[a]	20	57.80	5.26	$P=0.00$ (There are different meanings)
	1.5 (2)[a]	20	58.03	3.91	
	2 (3)[b]	20	59.82	3.67	
	Total	60			
Time (s)	90 (A)[a]	15	14.04	3.64	
	120 (B)[b]	15	18.56	7.04	
	150 (C)[c]	15	24.41	4.20	
	180 (D)[c]	15	27.45	6.28	
	Total	60			
Interaction	1A [(a)]	5	60.60	3.11	
	1B [(b,c)]	5	64.35	3.04	
	1C [(d,e)]	5	67.86	4.77	
	1D [(e,f)]	5	70.90	4.09	
	2A [(a,b)]	5	61.54	2.88	
	2B [(c,d)]	5	66.45	2.54	
	2C [(d,e)]	5	68.25	2.70	
	2D [(d,e)]	5	76.44	4,61	
	3A [(a,b)]	5	62.32	3,64	
	3B [(d,e)]	5	69.18	4,63	
	3C [(f)]	5	73.86	2.91	
	3D [(f)]	5	79.87	4.92	
Total		60			

* Description: N = number of samples. SD = standard deviation. The same superscript indicates a non-significant difference from the Tukey Post hoc test results.

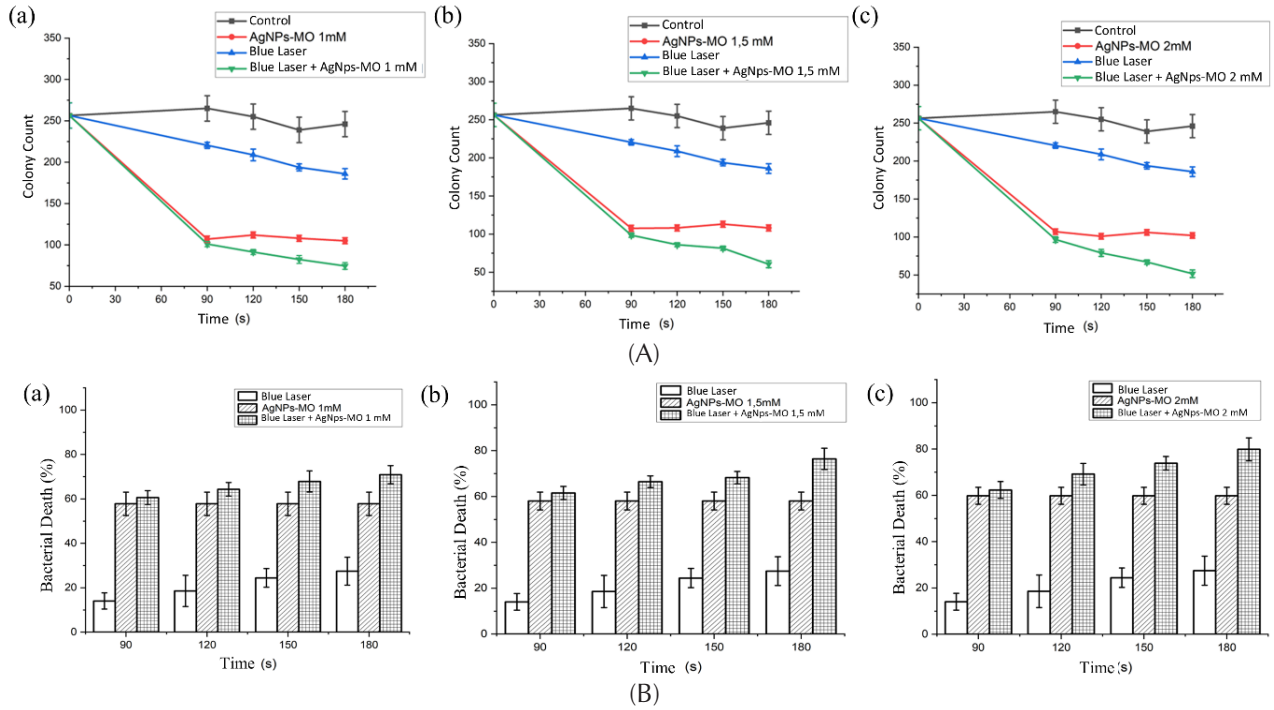

Figure 2. (A) Decreased viability of *E. coli* treated with AgNPs-MO at concentrations of mmol L^{-1} (a), mmol $L^{-1.5}$ (b), and mmol L^{-2} (c) without UV irradiation. (B) Percentage reduction of *E. coli* after treatment with AgNPs-MO at concentrations of mmol L^{-1} (a), mmol $L^{-1.5}$ (b), and mmol L^{-2} (c). The data show that increasing the AgNPs-MO concentration resulted in a progressive reduction in bacterial viability

Table 2. Results of statistical analysis on *S. aureus* bacteria

Treatment	Group	N	Bacterial Death (%)		Conclusion
			Mean	SD	
Concentration AgNPs-MO (mmol L)	1 (1)[a]	20	88.32	1.92	
	1.5 (2)[a]	20	87.34	1.92	
	2 (3)[b]	20	85.23	2.40	
Total		60			
Time (s)	90 (A)[a]	15	14.67	2.07	
	120 (B)[a,b]	15	19.22	3.70	
	150 (C)[b]	15	25.38	2,23	
	180 (D)[c]	15	29.19	2.96	
Total		60			
Interaction	1A [c,d,e,f]	5	94.24	2.03	$P=0.00$ (There are different meanings)
	1B [d,e]	5	94.89	1.85	
	1C [f]	5	96.97	1.35	
	1D [f]	5	97.48	1.72	
	2A [a,b]	5	91.07	2.73	
	2B [b,c]	5	92.78	1.92	
	2C [c,d,e]	5	93.91	1.58	
	2D [f]	5	95.94	2.23	
	3A [a]	5	90.10	2.60	
	3B [a,b]	5	91.80	2.58	
	3C [b,c,d]	5	92,94	1.94	
	3D [d,e,f]	5	94.72	2.54	
Total		60			

* Description: N = number of samples. SD = standard deviation. The same superscript indicates a non-significant difference from the Tukey Post hoc test results.

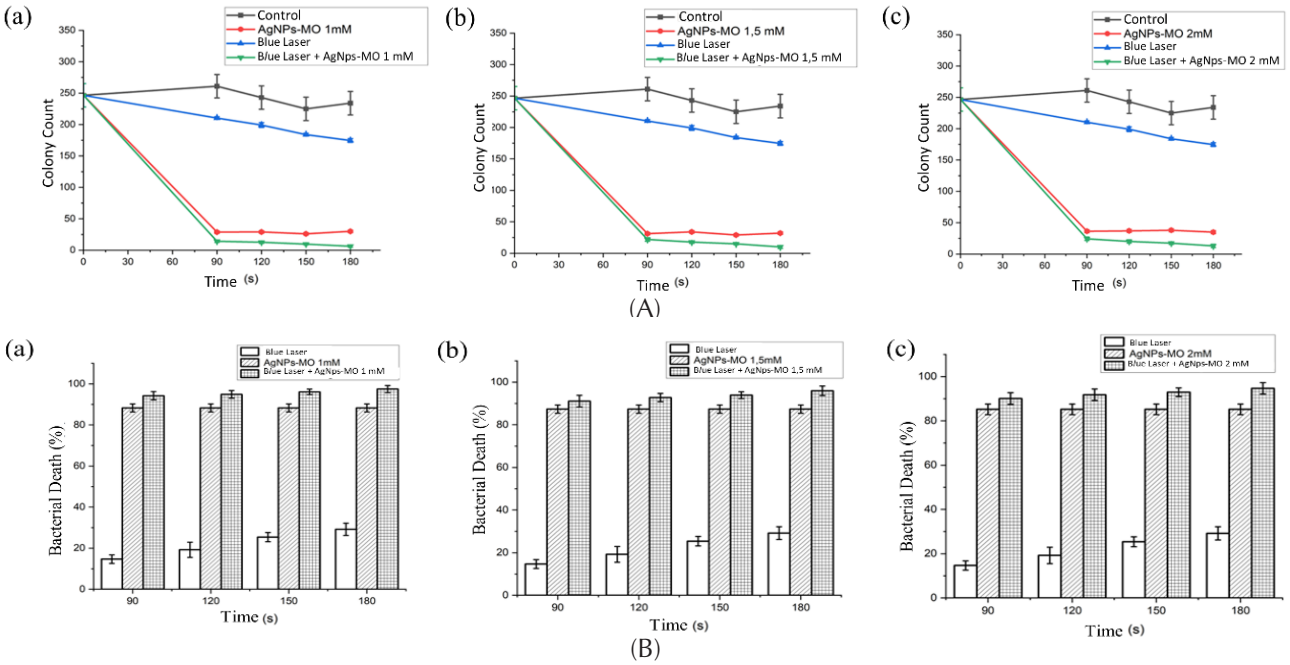

Figure 3. (A) Decreased viability of *S. aureus* treated with AgNPs-MO at concentrations of mmol L^{-1} (a), mmol $L^{-1.5}$ (b), and mmol L^{-2} (c). (B) Percentage reduction of *S. aureus* after treatment with AgNPs-MO at concentrations of mmol L^{-1} (a), mmol $L^{-1.5}$ (b), and mmol L^{-2} (c). The results demonstrate that higher concentrations of AgNPs-MO and longer laser exposure times enhanced bacterial inactivation

respectively. The results demonstrated that the 90, 120, 150, and 180-second time intervals had significantly different results. Table 2 displays the conclusions derived from the statistical test results. Figure 3A illustrates the decrease in viability of *S. aureus* following treatment with AgNPs-MO at concentrations of mmol L^{-1}, mmol $L^{-1.5}$, and mmol L^{-2}. A concentration-dependent reduction in bacterial viability was observed. Figure 3B presents the corresponding percentage reduction of *S. aureus* under the same AgNPs-MO concentrations, demonstrating increased antibacterial effectiveness with increasing concentration.

Table 2 shows the mean bacterial death (%) of *S. aureus* under varying concentrations of AgNPs-MO (mmol L^{-1}, mmol $L^{-1.5}$, and mmol L^{-2}), different laser exposure times (90, 120, 150, and 180 s), and their interactions. Each treatment group consisted of N replicates. The highest bacterial death (97.48%) occurred with 180-second laser exposure combined with mmol L^{-1} AgNPs-MO. Statistical analysis ($P<0.05$) confirms significant differences in bacterial mortality across the different treatments, demonstrating that increasing AgNPs-MO concentration and laser exposure time enhances bacterial inactivation.

Discussion

Microwave irradiation is a more efficient method for producing silver nanoparticles (AgNPs), which have improved antibacterial capabilities.[26] Photodynamic inactivation (PDI) targets and destroys bacterial cells while preserving Mammalian cells by producing reactive oxygen species (ROS). Blue diode lasers operating at a 405-nm wavelength enable accurate and productive photodynamic imaging (PDI) by providing steady output power and efficient creation of ROS.[27] The effectiveness of photodynamic treatment increases when nanoparticles and photosensitizers are combined, as this increases bacterial cell death by enhancing stability, cellular absorption, and ROS generation.[28]

The study investigates the use of microwave heating to create silver nanoparticles (AgNPs) containing Moringa oleifera extract, which improves photodynamic inactivation and reduces bacteria like S. aureus and *E. coli*. When combined with blue laser and UV irradiation, AgNPs-Moringa offers an eco-friendly alternative to antibiotics. Microwave heating is considered more effective than conventional heating due to its ability to produce uniformly sized nanoparticles with stronger antibacterial activity. The photoinactivation process occurs when the AgNPs-MO photosensitizer interacts with laser light.[29]

The photophysical mechanism that occurs when the AgNPs-MO photosensitizer interacts with the laser light source is what causes the photoinactivation process, as shown in Figure 4.

The photosensitizer's electron-level zone is where porphyrin molecules absorb photons, creating an excited singlet state. Intersystem crossover refers to the triplet excitation state resulting from electron spin interacting with excited singlet state electrons before exiting the

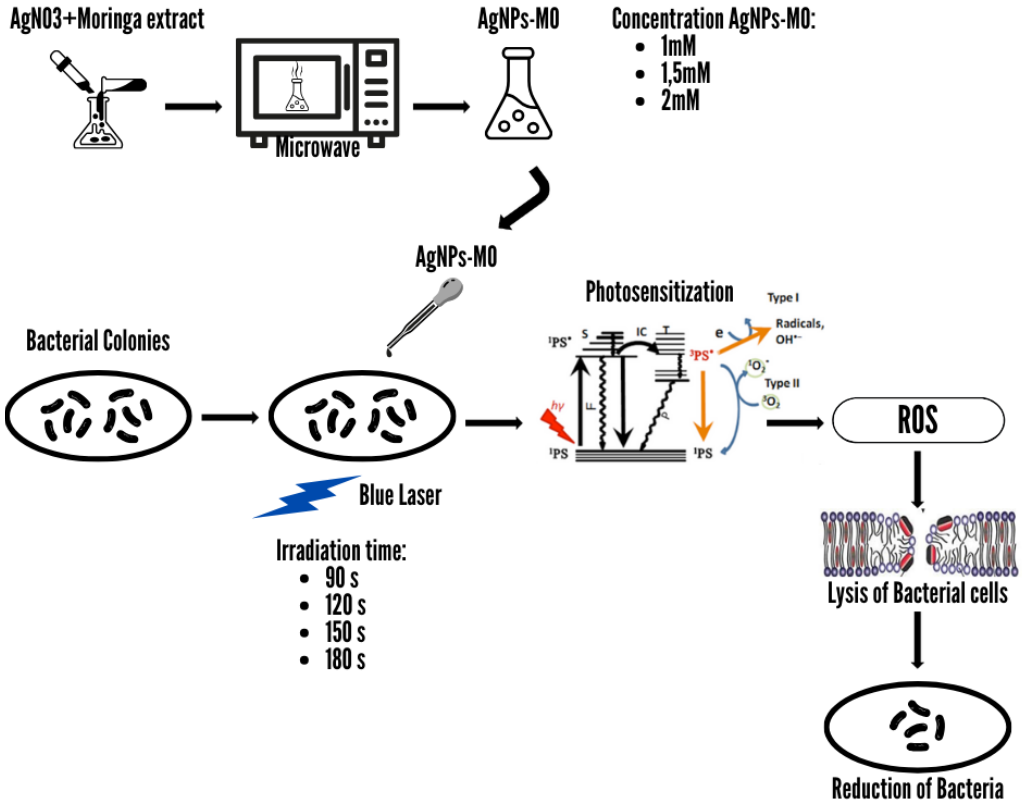

Figure 4. Bacterial inactivation mechanism

molecule, triggering a photochemical reaction.[30]

The photochemical process involves two types of pathways: type I and type II. Type I pathways allow excited sensitizers and biological molecules to exchange electrons, producing reactive oxygen species (ROS) and other radical ions.[31] These reactive oxygen species contribute to microbial cell damage and death, such as lipid peroxidation, which weakens the structural integrity of the bacterial cell wall[32]. In vitro studies are cost-effective and efficient methods for investigating phytocompounds of Moringa oleifera for treating MRSA.[33,34]

In this study, *E. coli* bacteria were used as gram-negative and *S. aureus* as gram-positive. Time variations of 90, 120, 150, and 180 seconds were applied in the irradiation process.[35, 36] Although the data analysis revealed a decrease in bacterial colonies and a rise in the percentage of bacterial death, no discernible change was found, especially at L1 and up to 150 seconds of irradiation. More reactive oxygen is produced during longer irradiation times, which raises the rate of bacterial mortality.[37, 38]

The results of studies on bacterial photoinactivation in *S. aureus* and *E. coli* bacteria revealed that photodynamic inactivation with a laser at 405 nm is more effective for *S. aureus* bacteria. Under dark conditions, laser irradiation of bacteria was performed for varying durations, specifically 90, 120, 150, and 180 seconds.[39,40,41] According to the findings of the irradiation studies, the maximum bacterial mortality rate was attained at a dosage of 3.44 J/cm^2 and an irradiation duration of 180 seconds.[42]

Antibiotic-resistant microorganisms have made infectious illnesses a serious health problem in Indonesia[43]. This work explores a novel approach to counter these bacteria by combining silver nanoparticles from Moringa oleifera (AgNPs-MO) with a blue laser with a wavelength of 405 nm.[44] The results demonstrated considerable declines in the viability of the bacteria, with *S. aureus* and *E. coli* showing declines of up to 97.48% and 79.87%, respectively, under certain circumstances.[45]

The chlorophyll-porphyrin complex is a light-harvesting vehicle when moringa-derived chlorophyll (MO extract) is combined with silver nanoparticles (AgNPs).[46] When combined, these porphyrin molecules improve the bactericidal effects of UV light, AgNPs, and 405 nm blue laser more than when employed alone.[47, 48, 49] The antibacterial activities of silver nanoparticles derived from Moringa oleifera (MO) extract increase, and the MO extract's dual purpose dramatically improves the stability and performance of the nanoparticles.[50,51]

In this study, the focus was primarily on confirming the antibacterial efficacy and ROS-mediated mechanism of blue laser-activated AgNPs synthesized using *Moringa oleifera* extract. Therefore, ROS quantification and colony reduction assays were prioritized to demonstrate the effectiveness of the treatment. Due to limited access to specialized flow cytometry equipment during the experimental period, this analysis could not be conducted. Nevertheless, future work will include flow cytometry or confocal microscopy to provide deeper insight into bacterial membrane integrity and cell death pathways following aPDT exposure.

The study reveals that AgNPs-MO, when combined with blue laser treatment, has the highest antibacterial activity. However, issues like opposition and uniformity need to be resolved before widespread use. The research aims to synthesize silver nanoparticles as photosensitizers for photodynamic therapy, which reduces pathogenic microbes by combining light with a photosensitizer agent to produce reactive oxygen species that damage bacterial cells. This green synthesis of nanoparticles has practical implications for medical applications.

Conclusion

Silver nanoparticles synthesized using Moringa oleifera extract (AgNPs-MO) inactivated bacteria effectively under blue laser (405 nm) irradiation. AgNPs-MO at 2 mmol·L^{-1} increased *E. coli* bacterial death by 59.82%, while 1 mmol·L^{-1} AgNPs-MO reduced *S. aureus* by 88.32%, showing higher efficacy against gram-positive bacteria. The combination of AgNPs-MO and laser treatment enhanced bacterial mortality through reactive oxygen species generation. Maximum bacterial death was achieved at an energy dose of 3.44 J·cm^{-2}. These findings indicate the potential of AgNPs-MO as a green photosensitizer for photodynamic antimicrobial therapy, though further studies are needed to assess long-term safety and environmental effects.

Acknowledgments

This research was supported by a grant from Indonesia Collaboration Research, No. 416/UN3/2023 and contract no. 955/UN3.LPPM/PT.01.03/2023.

Authors' Contribution

Conceptualization: Suryani Dyah Astuti, Endarko, Ahmad Khalil Yaqubi, Dezy Zahrotul Istiqomah Nurdin, Ardiansyah Syahrom
Data curation: Agustina Dwi Cahyani, Endarko, Muhammad Nurdin, Dezy Zahrotul Istiqomah Nurdin
Formal analysis: Agustina Dwi Cahyani, Sri Dewi Astuty, Muhammad Nurdin, Ardiansyah Syahrom
Investigation: Suryani Dyah Astuti, Agustina Dwi Cahyani, Ardiansyah Syahrom
Methodology: Suryani Dyah Astuti, Agustina Dwi Cahyani, Endarko.
Project administration: Suryani Dyah Astuti, Ahmad Khalil Yaqubi
Resources: Suryani Dyah Astuti, Endarko, Muhammad Nurdin, Ardiansyah Syahrom
Software: Agustina Dwi Cahyani, Sri Dewi Astuty, Dezy Zahrotul Istiqomah Nurdin
Supervision: Suryani Dyah Astuti
Validation: Suryani Dyah Astuti, Endarko, Ahmad Khalil Yaqubi
Visualization: Suryani Dyah Astuti, Sri Dewi Astuty, Ahmad Khalil Yaqubi, Dezy Zahrotul Istiqomah Nurdin
Writing–original draft: Agustina Dwi Cahyani
Writing–review & editing: Suryani Dyah Astuti, Ahmad Khalil Yaqubi

Competing Interests
The authors declare that there are no conflicts of interest.

Data Availability
The data used to support the findings of this study are available from the corresponding author upon reasonable request.

Ethical Approval
This clinical study has been approved by the Ethics Committee of Airlangga University Hospital (No. 130/KEP/2023) in accordance with the Indonesian Government's clinical trial guidelines. This study adhered to institutional biosafety protocols for the handling and disposal of *E. coli*, *S. aureus*, and silver nanoparticles (AgNPs). All materials were managed responsibly to minimize environmental impact and ensure safe containment and disposal.

Funding
This research was supported by a grant from Indonesia Collaboration Research, No. 416/UN3/2023.

Supplementary File
Supplementary file contains Tables S1-S2 and Figures S1-S3.

References
1. Fitri WN, Rahayu D. Antibacterial activity of Melastomataceae plant extracts against *Escherichia coli* and *S. aureus*. Farmaka. 2018;16(2):69-77.
2. Ministry of Health of the Republic of Indonesia. Indonesia Health Profile 2016: Bali Province Health Profile. Jakarta: Ministry of Health; 2016.
3. Mathesh A, Carmelin DS, Mohanprasanth A, Geetha Sravanthy P, Snega R, Surya M, et al. *Tridax procumbens*-mediated one pot synthesis of silver-doped fucoidan nanoparticles and their antibacterial, antioxidant, and anti-inflammatory efficacy. Biomass Convers Biorefin. 2024;14(8):9887-96. doi: 10.1007/s13399-023-05265-8
4. Saxena SK, Nyodu R, Kumar S, Maurya VK. Current advances in nanotechnology and medicine. In: Saxena SK, Khurana SM, eds. NanoBioMedicine. Singapore: Springer; 2020. p. 3-16. doi: 10.1007/978-981-32-9898-9_1
5. Deepak V, Umamaheshwaran PS, Guhan K, Nanthini RA, Krithiga B, Jaithoon NM, et al. Synthesis of gold and silver nanoparticles using purified URAK. Colloids Surf B Biointerfaces. 2011;86(2):353-8. doi: 10.1016/j.colsurfb.2011.04.019
6. Loza K, Diendorf J, Sengstock C, Ruiz-Gonzalez L, Gonzalez-Calbet JM, Vallet-Regi M, et al. The dissolution and biological effects of silver nanoparticles in biological media. J Mater Chem B. 2014;2(12):1634-43. doi: 10.1039/c3tb21569e
7. Girón-Vázquez NG, Gómez-Gutiérrez CM, Soto-Robles CA, Nava O, Lugo-Medina E, Castrejón-Sánchez VH, et al. Study of the effect of *Persea americana* seed in the green synthesis of silver nanoparticles and their antimicrobial properties. Results Phys. 2019;13:102142. doi: 10.1016/j.rinp.2019.02.078
8. Kumar B, Smita K, Cumbal L, Debut A, Pathak RN. Sonochemical synthesis of silver nanoparticles using starch: a comparison. Bioinorg Chem Appl. 2014;2014:784268. doi: 10.1155/2014/784268
9. Pareek A, Pant M, Gupta MM, Kashania P, Ratan Y, Jain V, et al. *Moringa oleifera*: an updated comprehensive review of its pharmacological activities, ethnomedicinal, phytopharmaceutical formulation, clinical, phytochemical, and toxicological aspects. Int J Mol Sci. 2023;24(3):2098. doi: 10.3390/ijms24032098
10. Khodashenas B, Ghorbani HR. Synthesis of silver nanoparticles with different shapes. Arab J Chem. 2019;12(8):1823-38. doi: 10.1016/j.arabjc.2014.12.014
11. Fatihin S, Harjono H, Kusuma SB. Synthesis of silver nanoparticles using bioreductant aquades extract of red guava fruit (*Psidium guajava* L.) and microwave irradiation. Indonesian Journal of Chemical Science. 2016;5(3):174-7.
12. Shankar SS, Rai A, Ahmad A, Sastry M. Rapid synthesis of Au, Ag, and bimetallic Au core-Ag shell nanoparticles using neem (*Azadirachta indica*) leaf broth. J Colloid Interface Sci. 2004;275(2):496-502. doi: 10.1016/j.jcis.2004.03.003
13. Anwar F, Latif S, Ashraf M, Gilani AH. *Moringa oleifera*: a food plant with multiple medicinal uses. Phytother Res. 2007;21(1):17-25. doi: 10.1002/ptr.2023
14. Salu V, Bernandus B, Bukit M. Preliminary study of the absorption spectrum of compounds from *Moringa* leaf extract (*Moringa oleifera* L.). Jurnal Fisika: Fisika Sains dan Aplikasinya. 2016;1(2):84-92. doi: 10.35508/fisa.v1i2.532
15. Elliott T, Casey A, Lambert PA, Sandoe J. Medical Microbiology and Infection. Wiley-Blackwell; 2011.
16. Sondi I, Salopek-Sondi B. Silver nanoparticles as antimicrobial agent: a case study on *E. coli* as a model for gram-negative bacteria. J Colloid Interface Sci. 2004;275(1):177-82. doi: 10.1016/j.jcis.2004.02.012
17. Ahmed E, El-Gendy AO, Moniem Radi NA, Mohamed T. The bactericidal efficacy of femtosecond laser-based therapy on the most common infectious bacterial pathogens in chronic wounds: an in vitro study. Lasers Med Sci. 2021;36(3):641-7. doi: 10.1007/s10103-020-03104-0
18. El-Gendy AO, Ezzat S, Samad FA, Dabbous OA, Dahm J, Hamblin MR, et al. Studying the viability and growth kinetics of vancomycin-resistant *Enterococcus faecalis* V583 following femtosecond laser irradiation (420-465 nm). Lasers Med Sci. 2024;39(1):144. doi: 10.1007/s10103-024-04080-5
19. El-Gendy AO, Obaid Y, Ahmed E, Enwemeka CS, Hassan M, Mohamed T. The antimicrobial effect of gold quantum dots and femtosecond laser irradiation on the growth kinetics of common infectious eye pathogens: an in vitro study. Nanomaterials (Basel). 2022;12(21):3757. doi: 10.3390/nano12213757
20. Astuti SD, Wibowo RA, Abdurachman NI, Triyana K. Antimicrobial photodynamic effects of polychromatic light activated by magnetic fields to bacterial viability. J Int Dent Med Res. 2017;10(1):111-7.
21. Karno K, Putra FP, Limantara JC. The effects of red and blue LED light on growth, yield and chlorophyll content of pakchoy (*Brassica chinensis* L.) plants in growbox. Agromix. 2022;13(2):168-74. doi: 10.35891/agx.v13i2.3028
22. Abadallah MS, Ali M. Antibacterial activity of *Moringa oleifera* leaf extracts against bacteria isolated from patients attending general Sani Abacha specialist hospital Damaturu. J Allied Pharm Sci. 2019;1(1):61-6.
23. Astuti SD, Kharisma DH, Kholimatussadiah S, Zaidan AH. An in vitro antifungal efficacy of silver nanoparticles activated by diode laser to *Candida albicans*. AIP Conf Proc. 2017;1888(1):020016. doi: 10.1063/1.5004293
24. Zaffer M, Ahmad S, Sharma R, Mahajan S, Gupta A, Agnihotri RK. Antibacterial activity of bark extracts of *Moringa oleifera* Lam. against some selected bacteria. Pak J Pharm Sci. 2014;27(6):1857-62.
25. Vairamuthu S, Sampath S, Sravanthy G, Surya M, Aruliah R, Ali H. Alshehri M, et al. Clove mediated synthesis of Ag-ZnO doped fucoidan nanocomposites and their evaluation of antibacterial, antioxidant and cytotoxicity efficacy study. Results Chem. 2024;11:101783. doi: 10.1016/j.rechem.2024.101783
26. Astuti SD, Hafidiana, Rulaningtyas R, Abdurachman, Putra AP, Samian, et al. The efficacy of photodynamic inactivation with

laser diode on *Staphylococcus aureus* biofilm with various ages of biofilm. Infect Dis Rep. 2020;12(Suppl 1):8736. doi: 10.4081/idr.2020.8736
27. Segwatibe MK, Cosa S, Bassey K. Antioxidant and antimicrobial evaluations of *Moringa oleifera* Lam leaves extract and isolated compounds. Molecules. 2023;28(2):899. doi: 10.3390/molecules28020899
28. Chandra J, Mukherjee PK, Ghannoum MA. Fungal biofilms in the clinical lab setting. Curr Fungal Infect Rep. 2010;4(3):137-44. doi: 10.1007/s12281-010-0020-z
29. Fouad N, Mahmoud A, Abdel Samad F, El-Salam YA, Ashour M, Apsari R, et al. Utilizing the 2nd harmonic Nd:YAG laser ablation in liquid for the production of copper oxide quantum dots: Influence of laser fluence and ablation duration. Physica B Condens Matter. 2024;694:416453. doi: 10.1016/j.physb.2024.416453
30. Basu C, Meinhardt-Wollweber M, Roth B. Lighting with laser diodes. Adv Opt Technol. 2013;2(4):313-21. doi: 10.1515/aot-2013-0031
31. Astuti SD, Prasaja BI, Prijo TA. An in vivo photodynamic therapy with diode laser to cell activation of kidney dysfunction. J Phys Conf Ser. 2017;853(1):012038. doi: 10.1088/1742-6596/853/1/012038
32. Kasithevar M, Periakaruppan P, Muthupandian S, Mohan M. Antibacterial efficacy of silver nanoparticles against multi-drug resistant clinical isolates from post-surgical wound infections. Microb Pathog. 2017;107:327-34. doi: 10.1016/j.micpath.2017.04.013
33. Mardianto AI, Setiawatie EM, Lestari WP, Rasheed A, Astuti SD. Photodynamic inactivation of *Streptococcus mutan* bacteri with photosensitizer *Moringa oleifera* activated by light emitting diode (LED). J Phys Conf Ser. 2020;1505(1):012061. doi: 10.1088/1742-6596/1505/1/012061
34. Ghaffari-Moghaddam M, Hadi-Dabanlou R, Khajeh M, Rakhshanipour M, Shameli K. Green synthesis of silver nanoparticles using plant extracts. Korean J Chem Eng. 2014;31(4):548-57. doi: 10.1007/s11814-014-0014-6
35. Rozykulyyeva L, Astuti SD, Zaidan AH, Pradhana AAS, Puspita PS. Antibacterial activities of green synthesized silver nanoparticles from *Punica granatum* peel extract. AIP Conf Proc. 2020;2314(1):060012. doi: 10.1063/5.0034126
36. Yaqubi AK, Astuti SD, Zaidan AH, Syahrom A, Nurdin DZ. Antibacterial effect of red laser-activated silver nanoparticles synthesized with grape seed extract against *Staphylococcus aureus* and *Escherichia coli*. Lasers Med Sci. 2024;39(1):47. doi: 10.1007/s10103-024-03991-7
37. Suhariningsih, Winarni D, Husen SA, Khaleyla F, Putra AP, Astuti SD. The effect of electric field, magnetic field, and infrared ray combination to reduce HOMA-IR index and GLUT 4 in diabetic model of *Mus musculus*. Lasers Med Sci. 2020;35(6):1315-21. doi: 10.1007/s10103-019-02916-z
38. Yaqubi AK, Astuti SD, Permatasari PA, Komariyah N, Endarko E, Zaidan AH. Effectiveness of purple LED for inactivation of *Bacillus subtilis* and *Escherichia coli* bacteria in in vitro sterilizers. Biomed Photonics. 2022;11(4):4-10. doi: 10.24931/2413–9432–2022–11-4-4-10
39. Kempa M, Kozub P, Kimball J, Rojkiewicz M, Kuś P, Gryczyński Z, et al. Physicochemical properties of potential porphyrin photosensitizers for photodynamic therapy. Spectrochim Acta A Mol Biomol Spectrosc. 2015;146:249-54. doi: 10.1016/j.saa.2015.03.076
40. Erdogan O, Abbak M, Demirbolat GM, Birtekocak F, Aksel M, Pasa S, et al. Green synthesis of silver nanoparticles via Cynara scolymus leaf extracts: The characterization, anticancer potential with photodynamic therapy in MCF7 cells. PLoS One. 2019;14(6):e0216496. doi: 10.1371/journal.pone.0216496
41. Babu N, Rahaman SA, John AM, Balakrishnan SP. Photosensitizer anchored nanoparticles: a potential material for photodynamic therapy. ChemistrySelect. 2022;7(17):e202200850. doi: 10.1002/slct.202200850
42. Baltazar LM, Ray A, Santos DA, Cisalpino PS, Friedman AJ, Nosanchuk JD. Antimicrobial photodynamic therapy: an effective alternative approach to control fungal infections. Front Microbiol. 2015;6:202. doi: 10.3389/fmicb.2015.00202
43. Sułek A, Pucelik B, Kobielusz M, Barzowska A, Dąbrowski JM. Photodynamic inactivation of bacteria with porphyrin derivatives: effect of charge, lipophilicity, ROS generation, and cellular uptake on their biological activity in vitro. Int J Mol Sci. 2020;21(22):8716. doi: 10.3390/ijms21228716
44. Vahidi H, Kobarfard F, Alizadeh A, Saravanan M, Barabadi H. Green nanotechnology-based tellurium nanoparticles: exploration of their antioxidant, antibacterial, antifungal and cytotoxic potentials against cancerous and normal cells compared to potassium tellurite. Inorg Chem Commun. 2021;124:108385. doi: 10.1016/j.inoche.2020.108385
45. Astuti SD, Utomo IB, Setiawatie EM, Khasanah M, Purnobasuki H, Arifianto D, et al. Combination effect of laser diode for photodynamic therapy with doxycycline on a Wistar rat model of periodontitis. BMC Oral Health. 2021;21(1):80. doi: 10.1186/s12903-021-01435-0
46. Aekthammarat D, Pannangpetch P, Tangsucharit P. *Moringa oleifera* leaf extract lowers high blood pressure by alleviating vascular dysfunction and decreasing oxidative stress in L-NAME hypertensive rats. Phytomedicine. 2019;54:9-16. doi: 10.1016/j.phymed.2018.10.023
47. Makita C, Chimuka L, Steenkamp P, Cukrowska E, Madala E. Comparative analyses of flavonoid content in *Moringa oleifera* and *Moringa ovalifolia* with the aid of UHPLC-qTOF-MS fingerprinting. S Afr J Bot. 2016;105:116-22. doi: 10.1016/j.sajb.2015.12.007
48. Bhagawan WS, Atmaja RR, Atiqah SN. Optimization and quercetin release test of *Moringa* leaf extract (*Moringa oleifera*) in gel-microemulsion preparation. J Islam Pharm. 2017;2(2):34-42. doi: 10.18860/jip.v2i2.4508
49. Jusnita N, Syurya W. Characterization of *Moringa* leaf extract nanoemulsion (*Moringa oleifera* Lamk). Jurnal Sains Farmasi Klinis. 2019;6(1):16-24.
50. Murga R, Ruiz R, Beltrán S, Cabezas JL. Extraction of natural complex phenols and tannins from grape seeds by using supercritical mixtures of carbon dioxide and alcohol. J Agric Food Chem. 2000;48(8):3408-12. doi: 10.1021/jf9912506
51. Nassiri-Asl M, Hosseinzadeh H. Review of the pharmacological effects of *Vitis vinifera* (grape) and its bioactive compounds. Phytother Res. 2009;23(9):1197-204. doi: 10.1002/ptr.2761